

Prognostic Value of Immune-Related IncRNA pairs in Patients with Bladder Cancer

zhenzhen Gao

The Second Affiliated Hospital of Jiaxing University

Dongjuan Wu

The Second Affiliated Hospital of Jiaxing University

Wenwen Zheng

The Second Affiliated Hospital of Jiaxing University

taohong Zhu

hospice center of jiaxing second hospital

Ting Sun

The Second Affiliated Hospital of Jiaxing University

Lianhong Yuan

The Second Affiliated Hospital of Jiaxing University

Faming Fei

The Second Affiliated Hospital of Jiaxing University

Peng Fu (✉ fupeng24@163.com)

The Second Affiliated Hospital of Jiaxing University <https://orcid.org/0000-0003-2982-6300>

Research

Keywords: bladder cancer, immunotherapy, long non-coding RNA, risk model, prognosis

Posted Date: August 3rd, 2021

DOI: <https://doi.org/10.21203/rs.3.rs-517245/v2>

License:   This work is licensed under a Creative Commons Attribution 4.0 International License.

[Read Full License](#)

Abstract

Background: The characteristics of immune-related long non-coding ribonucleic acids (ir-lncRNAs), regardless of their specific levels, have important implications for the prognosis of patients with bladder cancer.

Methods: Based on The Cancer Genome Atlas database, original transcript data were analyzed, the ir-lncRNAs were obtained using a coexpression method, and the differentially expressed pairs of ir-lncRNAs (DE-ir-lncRNAs) were identified by univariate analysis. The lncRNA pairs were verified using a Lasso regression test. Thereafter, receiver operating characteristic curves (ROC) were generated, area under the curve was calculated, Akaike information criterion of the 5-year ROC was determined, optimal cutoff value of the high- and low-risk populations of patients with bladder cancer was confirmed, and optimal risk model was established. The clinical value of the model was verified through the analysis of patient survival rates, clinicopathological characteristics, presence of tumor-infiltrating immune cells, and chemotherapy efficacy evaluation.

Results: In total, 49 pairs of DE-ir-lncRNAs were identified, of which 21 were included in the Cox regression model. A risk regression model was established on the premise of not involving the specific expression value of the transcripts.

Conclusions: The method and model used in this study have important clinical predictive value for bladder cancer and other malignant tumors.

Background

The incidence and mortality of bladder cancer (BLCA) are reported to be approximately 500,000 and 200,000 worldwide, respectively, in 2020[1]. Muscle-invasive bladder cancer (MIBC) accounts for approximately 25% of patients with BLCA[2]. Bacillus Calmette–Guérin, a type of *Mycobacterium*, reportedly prevent recurrence in patients with non-muscle-invasive bladder cancer, with the majority progressing to the MIBC subtype. Systemic chemotherapy has been the standard first-line therapy for MIBC, with patients who fail to respond to first-line treatments have few second-line chemotherapeutic options[3], including gemcitabine, paclitaxel, and ifosfamide, which have been associated with restricted clinical benefit. With the development of immune checkpoint inhibitors (ICIs), patients who have been treated with pembrolizumab as second-line therapy during the KEYNOTE045 trial[4] reportedly achieve approximately 10.3-month survival with an anti-tumor response (objective response rate) of 21.1%, which is greater than that in the chemotherapy group (11%). In addition, ICIs (atezolizumab and pembrolizumab) have also been confirmed to be effective as first-line therapy, based on the results of NCT02108652[5] and KEYNOTE052[6] phase II clinical trials. Therefore, the European Medicines Agency (EMA) as well as the U.S. Food and Drug Agency has approved atezolizumab and pembrolizumab as first-line treatments for metastatic cisplatin-ineligible MIBC, restricted to cisplatin-unfit patients with PD-

L1-high tumors. Although PD-L1 is a predictor of efficacy[7], other useful biomarkers related to ICIs for patients with BLCA need to be further explored to guide clinical practice.

Long non-coding RNAs (lncRNAs), with a transcript length of more than 200 nucleotides[8], do not encode proteins; however, they are abundant, occupying more than 80 human transcripts. With the development of advanced scientific methods, lncRNAs have been considered significant regulators of organic biological processes, including normal development and tumorigenesis. For example, the urothelial carcinoma-associated lncRNA (UCA1)[9], which was found to be overexpressed in BLCA compared with healthy tissues, was reportedly associated with cisplatin sensitivity by modulating miR-196a-5p via the regulation of CREB. Some lncRNAs have been reported to regulate the tumor microenvironment by targeting genes implicated in the function of immune cells[10–12]. Moreover, some immune-related lncRNA (ir-lncRNA) signatures have been recently identified in BLCA, and their expression was associated with the survival of patients with BLCA[13–15]. However, all these prognostic models were established based on the expression of lncRNA. Herein, we established a new model to predict the efficacy of immunotherapy regardless of expression.

Methods

RNA-seq data from The Cancer Genome Atlas (TCGA)-BLCA project were integrated into fragments per kilobase million (FPKM), and the GTF files were used to annotate and differentiate mRNAs and lncRNAs according to the Ensembl database (<http://asia.ensembl.org>). The ImmPort portal database (<http://www.immport.org>) was used to obtain confirmed immune-related genes and ir-lncRNAs by coexpression analysis. The relationship between immune-related genes and all lncRNAs was verified by correlation tests; the highly correlated lncRNAs were considered ir-lncRNAs, with the cutoff value of correlation efficacy being more than 0.5, and the P-value was ≤ 0.05 . Lastly, the R package “limma” (Bioconductor, USA) was used to detect differentially expressed lncRNAs (DE-lncRNAs), with the thresholds being defined as log fold change > 2 , with a false discovery rate < 0.05 .

For DE-ir-lncRNA pairing, if one of two markers was highly expressed in a sample, the sample was regarded as a highly expressing sample of the two DE-ir-lncRNA markers. DE-ir-lncRNAs were tautologically paired, and a 0 or 1 matrix was constructed as per the following rule: considering that A is equal to lncRNA B plus lncRNA C, A is 1 if the expression of lncRNA B is higher than that of lncRNA C; if not, A is defined as 0. The established matrix was filtered. Pairs were considered to not be related to prognosis as long the expression value of the lncRNA pair was 0 or 1. DE-lncRNA pairs were deemed to be an applicable match when the expression value was more than 20% of the total pairs.

The least absolute shrinkage and selection operator (Lasso) regression model[16] was constructed with a P-value of 0.05. The Lasso regression was performed for 1,000 cycles and, for each cycle, a random stimulation was set up 1,000 times. Afterward, the frequency of each pair in the 1,000-time-repeated Lasso regression model was recorded, and pairs with frequencies more than 100 times were selected for Cox proportional hazard regression analysis, as well as for the construction of the model. The area under

the curve (AUC) of each model was calculated and plotted as a curve. If the curve reached the highest point, indicating the maximum AUC value, the calculation procedure was terminated, and the model was considered the optimal candidate. Then, we conducted a Kaplan–Meier analysis to validate the accuracy of the risk model using the R packages[17] “survival,” “glmnet,” “pbapply,” “survivalROC,” “survminer,” and “heatmap.” Chi-square test was used to analyze the relationship between the risk model and clinical characteristics, and the Wilcoxon test was used to evaluate risk score differences among the clinical groups.

We applied novel methods to calculate the immune infiltration status among BLCA, including TIMER (<http://cistrome.org/TIMER/>), CIBERSORT, XCELL, QUANTISEQ, MCPcounter, and EPIC. The Wilcoxon signed-rank test was then applied to calculate the differences in infiltrating immune cells between the high- and low-risk groups. Subsequently, the relationship between the risk score values and the immune-infiltrated cells was evaluated using Spearman’s correlation analysis. The significance cutoff was set at $P < 0.05$. The R package “ggplot2” was used for this analysis.

Finally, we calculated the half-maximal inhibitory concentration (IC50) of common chemotherapeutic drugs among patients with BLCA in the TCGA-BLCA project. The difference between the high- and low-risk groups was determined using the Wilcoxon test, and results were obtained using the R packages “pRRophetic” and “ggplot2.”

Results

Identification of DE-ir-lncRNAs and construction of two DE-ir-lncRNA pairs

A flow chart of the study is shown in Fig. 1. First, we identified the raw data for BLCA from the TCGA project, which comprised 19 normal and 411 tumor samples. Then, we annotated the transcriptome according to the Ensembl database. A total of 1,269 ir-lncRNAs were detected (Table S1), among which 109 were identified as DE-ir-lncRNAs, (14 downregulated and 95 upregulated; Fig. 2A). Ultimately, we constructed a 0 or 1 matrix to generate DE-ir-lncRNA pairs. In total, 4,896 pairs were constructed, 251 pairs were identified using univariate analysis, and 49 DE-ir-lncRNA pairs were verified by Lasso regression model analysis. We established a multi-Cox regression model including 21 DE-lncRNA pairs using the forward method (Fig. 2B).

Establishing a risk assessment model and evaluating its relationship with prognosis of patients with BLCA

Subsequently, we calculated the AUCs for each receiver operating characteristic (ROC) curve for the 21 DE-lncRNA pairs (Fig. 3A) and detected the optimal cutoff value, which referred to 1,483 using the Akaike information criterion[18] (AIC) values[19] (Fig. 3B). Based on the cutoff point, we divided the patients into high- and low-risk groups. To validate the cutoff value, we delineated the 1-, 3-, and 5-year ROC curves, the

AUC values of which were over 0.80 (Fig. 3C), and outlined the 5-year ROC curves with other clinical characteristics (Fig. 3D).

Evaluating the relationship between the risk assessment model and clinical characteristics

Based on the cutoff value previously defined, 156 and 244 patients were categorized into the high- and low-risk groups, respectively. Risk scores and survival data of each patient are shown in Figs. 4A and 4B, confirming that the clinical prognosis of the low-risk group was superior to that of the high-risk group. Moreover, we observed that patients in the low-risk group had longer survival than those in the high-risk group, according to analysis using the Kaplan–Meier method ($P < 0.0001$) (Fig. 4C). Subsequently, we conducted chi-square tests to elucidate the relationship between the risk of BLCA and clinical characteristics. The ribbon chart and ladder diagrams established using the Wilcoxon signed-rank test showed that age (Fig. 5B), grade (Fig. 5C), and stage (Fig. 5D) were significantly associated with the risk group ($P < 0.001$). Moreover, age ($P < 0.01$, hazard ratio (HR) = 1.026, 95% confidence interval (CI) [1.009–1.042]), stage ($P < 0.001$, HR = 1.564, 95% CI [1.280–1.912]), and risk score ($P < 0.001$, HR = 1.154, 95% CI [1.126–1.182]) were statistically significant as indicated by univariate Cox regression model analysis (Fig. 5E), and further verified by multivariate Cox regression analysis.

Relationship Between The Tumor Microenvironment And The Risk Model

After establishing and verifying the risk model, we investigated whether the model was relevant to the tumor immune microenvironment. The high-risk group was more significantly associated with tumor-infiltrating immune cells, such as macrophages, neutrophils, and CD8⁺ T-cells, but negatively associated with myeloid dendritic cells and CD4⁺ T-cells, as verified using the Wilcoxon signed-rank test (Fig. 6A). As ICIs have been used to treat BLCA in clinical practice, we investigated whether the risk model was correlated with ICI-related biomarkers. Overall, high-risk scores were positively correlated with the high expression of discoidin domain receptor tyrosine kinase 2 (*DDR2*) ($P < 0.05$, Fig. 6C) and hepatitis A virus cellular receptor 2 (*HAVCR2*) ($P < 0.001$, Fig. 6D), whereas lymphocyte activating 3 (*LAG3*) ($P > 0.05$, Fig. 6E) and cytotoxic T-lymphocyte associated protein 4 (*CTLA4*) ($P > 0.05$, Fig. 6A) showed no significant differences.

Relationship Between The Risk Model And Clinical Chemotherapeutics

In addition to the aforementioned immunotherapy, we identified the potential relationship between the risk model and the efficacy of common chemotherapeutics in treating BLCA. The analysis of the TCGA-BLCA dataset revealed that a high-risk score was associated with a lower IC₅₀ of chemotherapeutics, such as cisplatin ($P = 0.00021$, Fig. 7A), docetaxel ($P < 0.0001$, Fig. 7B), and paclitaxel ($P < 0.0047$,

Fig. 7C). In contrast, we found that it was associated with a higher IC50 for metformin ($P < 0.001$, Fig. 7D) and methotrexate ($P < 0.001$, Fig. 7E). Collectively, these results demonstrate the predictive value of the proposed DE-lncRNA-based risk model.

Discussion

It is well known that the expression of lncRNAs has crucial biological functions. Some of the DE-ir-lncRNAs detected in this study, such as TRPM2-AS, LINC01605, AC104041.1, and UCA1, have been confirmed to play significant roles in the progression of BLCA. Avgeris *et al.*[20] reported that the downregulation of UCA1 was correlated with a higher risk of short-term relapse in BLCA. Tian *et al.*[21] reported that TRPM2-AS promoted BLCA by targeting miR-22-3p and regulating the expression of *GINS2*. Qin *et al.*[22] revealed that high LINC01605 expression promoted the progression of BLCA by upregulating MMP9. Moreover, Lian *et al.*[23] established an 8-lncRNA signature, comprising APCDD1L-AS1, FAM225B, LINC00626, LINC00958, LOC100996694, LOC441601, LOC101928111, and ZSWIM8-AS1, as candidate prognostic markers for BLCA. Although various functions of lncRNAs have been proposed, single lncRNAs may have a bias to predict the prognosis of patients with BLCA. Previous studies[24, 25] have shown that the combinations of two genetic markers are more accurate than single genes in establishing prognostic models for cancers. To date, few studies have confirmed the prognostic value of lncRNA pairs in this setting[26–28]. In the present study, we established a prognostic risk model by pairing immune-related genes and constructed a risk model with two lncRNA pairs, without adopting their exact expression value. First, we screened the lncRNAs within the TCGA-BLCA dataset, selected the DE-lncRNAs, conducted a coexpression analysis to identify the DE-ir-lncRNAs, and validated the obtained DE-ir-lncRNA-pairs using a 0-or-1 matrix. Second, we applied a modified Lasso penalized regression model, including the procedures of the cross, multiple repetitions of validation, and random stimulations to determine DE-ir-lncRNA pairs. Third, we delineated ROC curves and calculated the AUC values to acquire the optimized model. In addition, we calculated the AIC value of each point on the AUC to detect the best cutoff value to differentiate the high- and low-risk groups among patients with BLCA. Finally, we assessed the relationship between this novel risk model and different clinical parameters.

Preclinical studies have confirmed that increased infiltration of CD4⁺ or CD8⁺ immune cells[29–31] leads to a better response to ICIs. In the present study, we used various online tools, including CIBERSORT, XCELL, CIBERSORT-ABS, QUANTISEQ, MCPcounter, EPIC, and TIMER, to estimate the tumor-infiltrating cells in patients with BLCA, and analyzed their association with the predicted risk scores. Our results showed that CD4⁺ T-cells, monocytes, macrophages, cancer-associated fibroblasts, and myeloid dendritic cells were enriched in the high-risk group, which may explain why the high-risk group was related to poor prognosis. In addition, correlation analysis demonstrated that the high-risk group was positively correlated with the expression of some immune microenvironmental inhibitory genes, such as *HAVCR2*, *DDR2*, and a positive correlation trend with *LAG3*.

LINC00665 and some other lncRNAs have been shown to enhance the efficacy of immunotherapy in BLCA[32–34]. In addition, Zhang *et al.*[35] found that the lncRNA HOTAIR can inhibit 5-fluorouracil

sensitivity by mediating *MTHFR* methylation, and Gu *et al.* reported that NONHSAT141924 was associated with paclitaxel chemotherapy resistance[36]. Overall, these findings demonstrate that lncRNAs may be related to chemotherapy resistance. Based on this, herein, we explored the relationship between the identified risk group and chemotherapy. Our risk model suggested that the high-risk group was more sensitive to methotrexate and metformin, whereas the low-risk group was more sensitive to cisplatin, docetaxel, and paclitaxel, which was consistent with previous studies.

There were some limitations to our study. First, the raw data obtained from the TCGA database were relatively insufficient for an initial analysis. Second, external validation was necessary to verify the efficiency of the risk model herein established. To overcome these limitations, we screened lncRNA pairs using a 0-or-1 matrix, which was optimal in this study. Further studies comprising more clinical samples are underway for further verification of the proposed model. In summary, we defined a novel risk predictive model comprising ir-lncRNAs that does not require the exact expression of the lncRNAs, which may help clinicians identify patients who can benefit from immunotherapy.

Conclusions

In the study, we established a lncRNA pair model with the exact expression to predict the prognosis of patients with bladder cancer, which may have significant value for clinical practice.

Abbreviations

AIC, Akaike information criterion; AUC, area under the curve; BLCA, bladder cancer; CI, confidence interval; DE-lncRNAs, differentially expressed lncRNAs; IC50, half-maximal inhibitory concentration; ICI, immune checkpoint inhibitor; ir-lncRNA, immune-related lncRNA; lncRNAs, long non-coding RNAs; MIBC, muscle-invasive bladder cancer; ROC, receiver operating characteristic; TCGA, The Cancer Genome Atlas; UCA1, urothelial carcinoma-associated lncRNA.

Declarations

Ethics approval and consent to participate

All analyses were based on publicly available online datasets, thus no ethical approval and patient consent were required.

Consent for publication

Not applicable.

Availability of data and materials

All data used in this study is publicly available in online database.

Competing interests:

The authors declare no potential conflicts of interest concerning the research, authorship, and/or publication of this article.

Funding

Financial support was provided by the Jiaxing Science and Technology Bureau (2021AD3017 and 2020AD30084), and the Medical and Health Science and Technology Project of the Zhejiang Province (2021KY354).

Authors' contributions

Z. Gao was responsible for the design. P. Fu and F.M. Fei provided the administrative support. T. Sun and T.H. Zhu were responsible for the collection and assembly of the data. L.H. Yuan, D.J. Wu, W.W. Zheng, and Z. Gao were responsible for writing the manuscript. All authors approved the final manuscript. Our study did not require an ethical board approval because it did not contain human or animal trials.

Acknowledgments

We thank the support of the Dean of the Jiaxing Second Hospital (G. Chen).

Authors' information

¹ Department of Clinical Oncology, The Second Affiliated Hospital of Jiaxing University, Jiaxing, China. ² Department of General Medicine, Nanhu District Central Hospital of Jiaxing, Jiaxing, China. ³ Department of Orthopedic Oncology, The Second Affiliated Hospital of Jiaxing University, Jiaxing, China. ⁴ Hospice Care Center, Jiaxing Second Hospital, Jiaxing, China.

References

1. Afonso J, Santos LL, Longatto-Filho A, Baltazar F. Competitive glucose metabolism as a target to boost bladder cancer immunotherapy. *Nature reviews Urology*. 2020;17(2):77–106. 10.1038/s41585-019-0263-6.
2. Autio KA, Boni V, Humphrey RW, Naing A. Probody Therapeutics: An Emerging Class of Therapies Designed to Enhance On-Target Effects with Reduced Off-Tumor Toxicity for Use in Immuno-Oncology. *Clinical cancer research: an official journal of the American Association for Cancer Research* 2020, 26(5):984–9. 10.1158/1078 – 0432.Ccr-19-1457.
3. Benitez JC, Remon J, Besse B. Current Panorama and Challenges for Neoadjuvant Cancer Immunotherapy. *Clinical cancer research: an official journal of the American Association for Cancer Research*. 2020;26(19):5068–77. 10.1158/1078 – 0432.Ccr-19-3255.

4. Fradet Y, Bellmunt J, Vaughn DJ, Lee JL, Fong L, Vogelzang NJ, et al. Randomized phase III KEYNOTE-045 trial of pembrolizumab versus paclitaxel, docetaxel, or vinflunine in recurrent advanced urothelial cancer: results of > 2 years of follow-up. *Ann Oncol*. 2019;30(6):970–6. 10.1093/annonc/mdz127.
5. Snyder A, Nathanson T, Funt SA, Ahuja A, Buros Novik J, Hellmann MD, et al. Contribution of systemic and somatic factors to clinical response and resistance to PD-L1 blockade in urothelial cancer: An exploratory multi-omic analysis. *PLoS Med*. 2017;14(5):e1002309. 10.1371/journal.pmed.1002309.
6. Jacqueline Vuky AVB, Bellmunt J, Fang X, Plimack ER, Castellano D, Godwin JL, Powles T, Bajorin D, Frenkl TL, Peter H, O'Donnell NM, Hahn BH, Moreno,, ; Petros Grivas MJS. Ronald de Wit. Long-Term Outcomes in KEYNOTE-052: Phase II Study Investigating First-Line Pembrolizumab in Cisplatin-Ineligible Patients With Locally Advanced or Metastatic Urothelial Cancer. *J Clin Oncol*. 2020;38(23):2658–66.
7. Tran L, Xiao JF, Agarwal N, Duex JE, Theodorescu D. Advances in bladder cancer biology and therapy. *Nat Rev Cancer*. 2021;21(2):104–21. 10.1038/s41568-020-00313-1.
8. Linxweiler J, Junker K. Extracellular vesicles in urological malignancies: an update. *Nature reviews Urology*. 2020;17(1):11–27. 10.1038/s41585-019-0261-8.
9. Pan J, Li X, Wu W, Xue M, Hou H, Zhai W, et al. Long non-coding RNA UCA1 promotes cisplatin/gemcitabine resistance through CREB modulating miR-196a-5p in bladder cancer cells. *Cancer Lett*. 2016;382(1):64–76. 10.1016/j.canlet.2016.08.015.
10. Chen C, He W, Huang J, Wang B, Li H, Cai Q, et al. LNMAT1 promotes lymphatic metastasis of bladder cancer via CCL2 dependent macrophage recruitment. *Nature communications*. 2018;9(1):3826. 10.1038/s41467-018-06152-x.
11. Chen C, Luo Y, He W, Zhao Y, Kong Y, Liu H, et al. Exosomal long noncoding RNA LNMAT2 promotes lymphatic metastasis in bladder cancer. *J Clin Investig*. 2020;130(1):404–21. 10.1172/jci130892.
12. Chen X, Xie R, Gu P, Huang M, Han J, Dong W, et al. Long Noncoding RNA LBCS Inhibits Self-Renewal and Chemoresistance of Bladder Cancer Stem Cells through Epigenetic Silencing of SOX2. *Clinical cancer research: an official journal of the American Association for Cancer Research* 2019, 25(4):1389–403. 10.1158/1078 – 0432.Ccr-18-1656.
13. Zhan Y, Chen Z, He S, Gong Y, He A, Li Y, et al. Long non-coding RNA SOX2OT promotes the stemness phenotype of bladder cancer cells by modulating SOX2. *Mol Cancer*. 2020;19(1):25. 10.1186/s12943-020-1143-7.
14. Zhan Y, Du L, Wang L, Jiang X, Zhang S, Li J, et al. Expression signatures of exosomal long non-coding RNAs in urine serve as novel non-invasive biomarkers for diagnosis and recurrence prediction of bladder cancer. *Mol Cancer*. 2018;17(1):142. 10.1186/s12943-018-0893-y.
15. Zheng R, Du M, Wang X, Xu W, Liang J, Wang W, et al. Exosome-transmitted long non-coding RNA PTENP1 suppresses bladder cancer progression. *Mol Cancer*. 2018;17(1):143. 10.1186/s12943-018-0880-3.

16. TIBSHIRANI R. THE LASSO METHOD FOR, VARIABLE SELECTION IN THE COX MODEL. *STATISTICS IN MEDICINE* 1997, 16:385–95.
17. Robert C, Gentleman VJC, Douglas M, Bates B, Bolstad M, Dettling S, Dudoit B, Ellis L, Gautier Y, Ge J, Gentry K, Hornik T, Hothorn W, Huber S, Iacus R, Irizarry F, Leisch C, Li M, Maechler AJ, Rossini. Gunther Sawitzki, Colin Smith, Gordon Smyth, Luke Tierney, Jean YH Yang and Jianhua Zhang. *Bioconductor: open software development for computational biology and bioinformatics. Genome Biol.* 2004;5(10):80–6.
18. Posada D, Buckley TR. Model selection and model averaging in phylogenetics: advantages of akaike information criterion and bayesian approaches over likelihood ratio tests. *Syst Biol.* 2004;53(5):793–808. 10.1080/10635150490522304.
19. Vrieze SI. Model selection and psychological theory: a discussion of the differences between the Akaike information criterion (AIC) and the Bayesian information criterion (BIC). *Psychol Methods.* 2012;17(2):228–43. 10.1037/a0027127.
20. Avgeris M, Tsilimantou A, Levis PK, Rampias T, Papadimitriou MA, Panoutsopoulou K, et al. Unraveling UCA1 lncRNA prognostic utility in urothelial bladder cancer. *Carcinogenesis.* 2019;40(8):965–74. 10.1093/carcin/bgz045.
21. Tian Y, Guan Y, Su Y, Yang T, Yu H. TRPM2-AS Promotes Bladder Cancer by Targeting miR-22-3p and Regulating GINS2 mRNA Expression. *Onco Targets Ther.* 2021;14:1219–37. 10.2147/OTT.S282151.
22. Qin Z, Wang Y, Tang J, Zhang L, Li R, Xue J, et al. High LINC01605 expression predicts poor prognosis and promotes tumor progression via up-regulation of MMP9 in bladder cancer. *Biosci Rep* 2018, 38(5). 10.1042/BSR20180562.
23. Penghu Lian QW, Zhao Y, Chen C, Sun X, Li H, Deng J, Zhang H, Ji Z, Zhang X. Qichao Huang. An eight-long non-coding RNA signature as a candidate prognostic biomarker for bladder cancer. *Aging,* 11:6930–6940.
24. Hendriks RJ, Dijkstra S, Smit FP, Vandersmissen J, Van de Voorde H, Mulders PFA, et al. Epigenetic markers in circulating cell-free DNA as prognostic markers for survival of castration-resistant prostate cancer patients. *Prostate.* 2018;78(5):336–42. 10.1002/pros.23477.
25. Liu X, Wang J, Chen M, Liu S, Yu X, Wen F. Combining data from TCGA and GEO databases and reverse transcription quantitative PCR validation to identify gene prognostic markers in lung cancer. *Onco Targets Ther.* 2019;12:709–20. 10.2147/OTT.S183944.
26. Wu Y, Zhang L, He S, Guan B, He A, Yang K, et al. Identification of immune-related lncRNA for predicting prognosis and immunotherapeutic response in bladder cancer. *Aging.* 2020;12(22):23306–25. 10.18632/aging.104115.
27. Robertson AG, Kim J, Al-Ahmadie H, Bellmunt J, Guo G, Cherniack AD, et al. Comprehensive Molecular Characterization of Muscle-Invasive Bladder Cancer. *Cell.* 2017;171(3):540–56 e525. 10.1016/j.cell.2017.09.007.
28. Zhou M, Zhang Z, Bao S, Hou P, Yan C, Su J, et al. Computational recognition of lncRNA signature of tumor-infiltrating B lymphocytes with potential implications in prognosis and immunotherapy of

- bladder cancer. *Brief Bioinform.* 2020. 10.1093/bib/bbaa047.
29. Elizabeth Pluhara G. CAP, and Michael R. Olin. CD8 + T Cell-Independent Immune-Mediated Mechanisms of AntiTumor Activity. *Crit Rev Immunol*, 35(2):153–172.
 30. Ostroumov D, Fekete-Drimusz N, Saborowski M, Kuhnel F, Woller N. CD4 and CD8 T lymphocyte interplay in controlling tumor growth. *Cell Mol Life Sci.* 2018;75(4):689–713. 10.1007/s00018-017-2686-7.
 31. Tay RE, Richardson EK, Toh HC. Revisiting the role of CD4(+) T cells in cancer immunotherapy-new insights into old paradigms. *Cancer Gene Ther.* 2021;28(1–2):5–17. 10.1038/s41417-020-0183-x.
 32. Zhang Y, Liu Q, Liao Q. Long noncoding RNA: a dazzling dancer in tumor immune microenvironment. *J Exp Clin Cancer Res.* 2020;39(1):231. 10.1186/s13046-020-01727-3.
 33. Cong Z, Diao Y, Xu Y, Li X, Jiang Z, Shao C, et al. Long non-coding RNA linc00665 promotes lung adenocarcinoma progression and functions as ceRNA to regulate AKR1B10-ERK signaling by sponging miR-98. *Cell Death Dis.* 2019;10(2):84. 10.1038/s41419-019-1361-3.
 34. Yang D, Feng W, Zhuang Y, Liu J, Feng Z, Xu T, et al. Long non-coding RNA linc00665 inhibits CDKN1C expression by binding to EZH2 and affects cisplatin sensitivity of NSCLC cells. *Mol Ther Nucleic Acids.* 2021;23:1053–65. 10.1016/j.omtn.2021.01.013.
 35. Zhang S, Zheng F, Zhang L, Huang Z, Huang X, Pan Z, et al. LncRNA HOTAIR-mediated MTHFR methylation inhibits 5-fluorouracil sensitivity in esophageal cancer cells. *J Exp Clin Cancer Res.* 2020;39(1):131. 10.1186/s13046-020-01610-1.
 36. Gu M, Zheng W, Zhang M, Dong X, Zhao Y, Wang S, et al. LncRNA NONHSAT141924 promotes paclitaxel chemotherapy resistance through p-CREB/Bcl-2 apoptosis signaling pathway in breast cancer. *J Cancer.* 2020;11(12):3645–54. 10.7150/jca.39463.

Figures

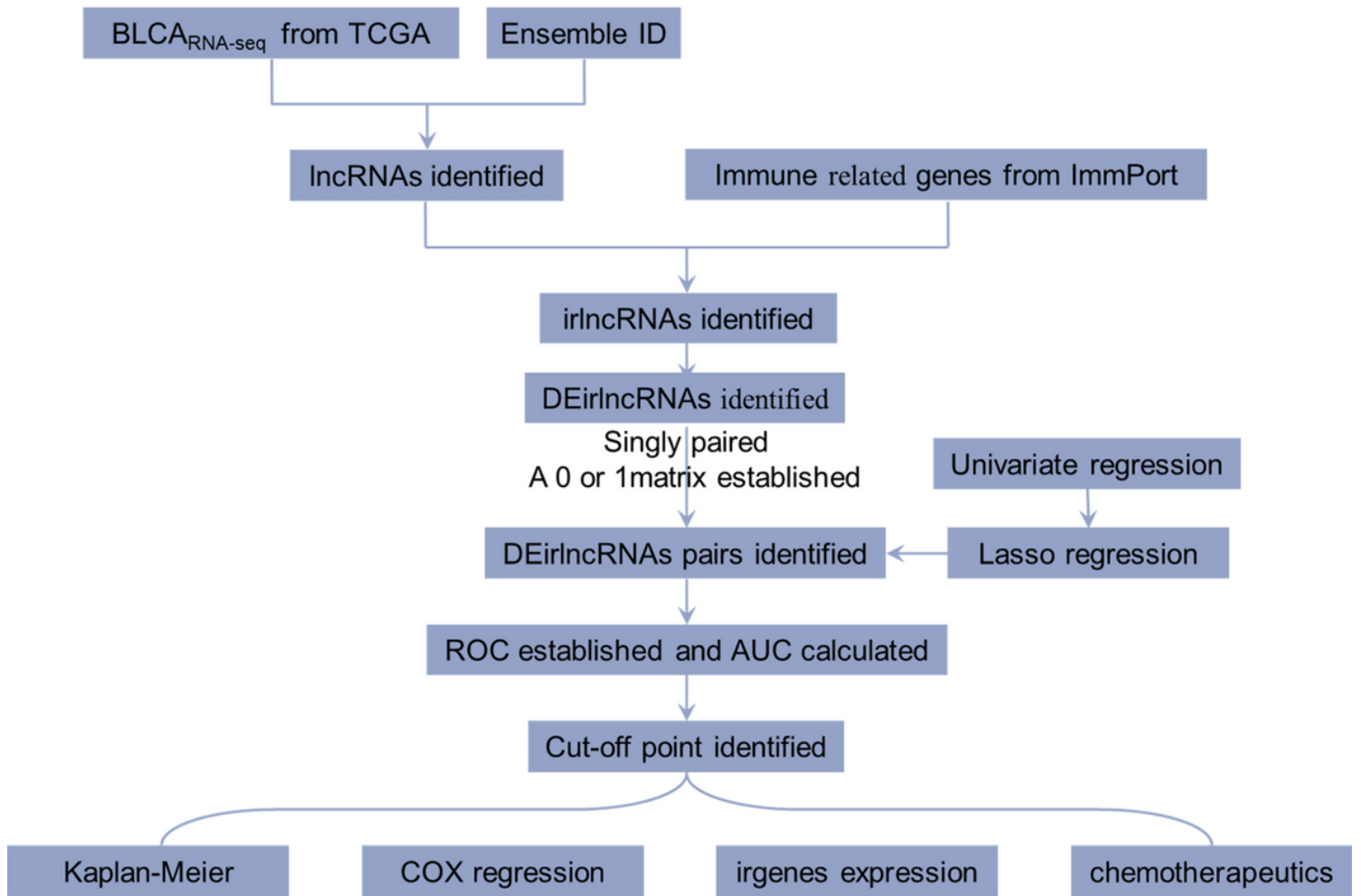


Figure 1

Detailed flow chart of the study approach.

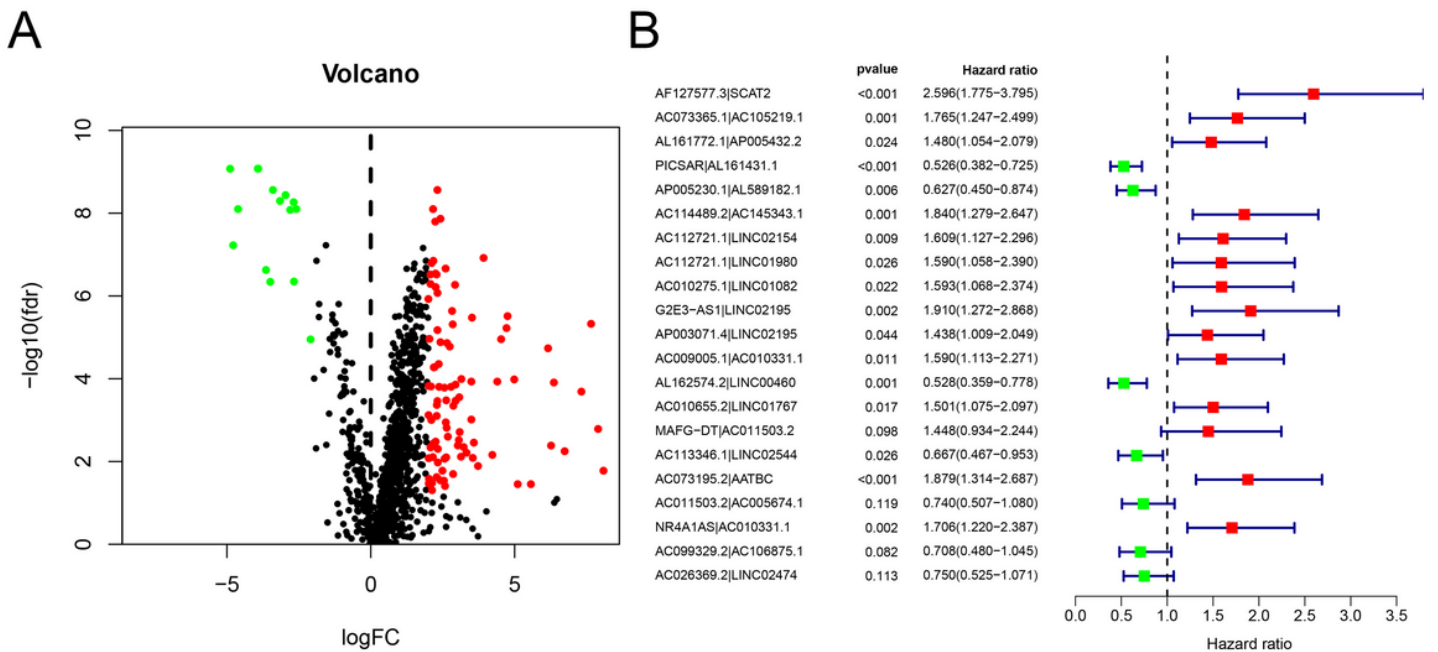


Figure 2

Detection of DE-ir-lncRNAs (A) and identification of 21 DE-lncRNAs by COX regression model (B).

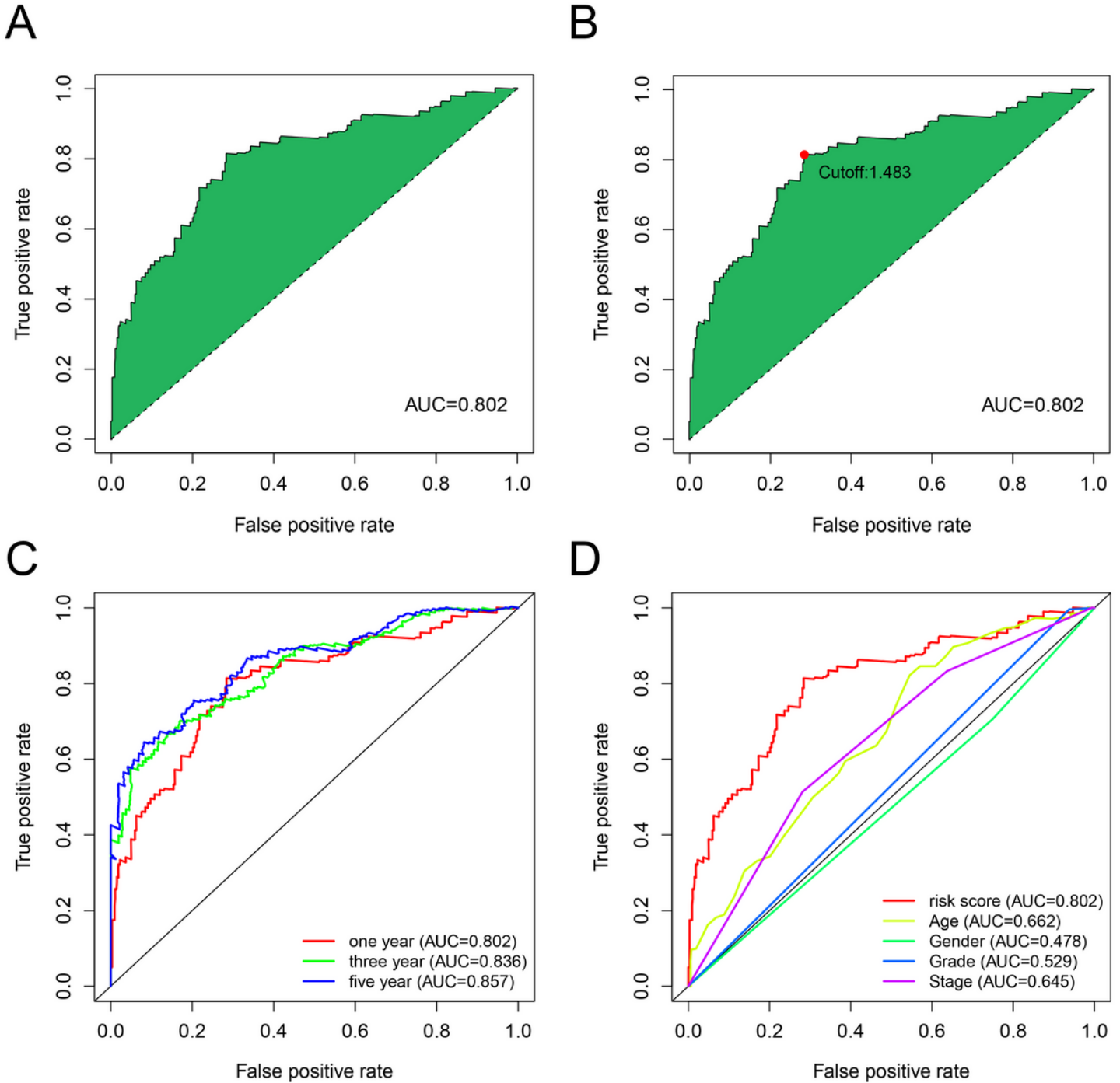


Figure 3

Proposed model comprising 21 DE-ir-lncRNA pairs related to the optimal AUC (A). All AUC values of the model were over 0.80 (B). AUC of 1-year ROC curves was compared with common clinical characteristics (C). RiskScore (E) for 430 patients with BLCA, and cut-off point shown in this figure were obtained by the AIC.

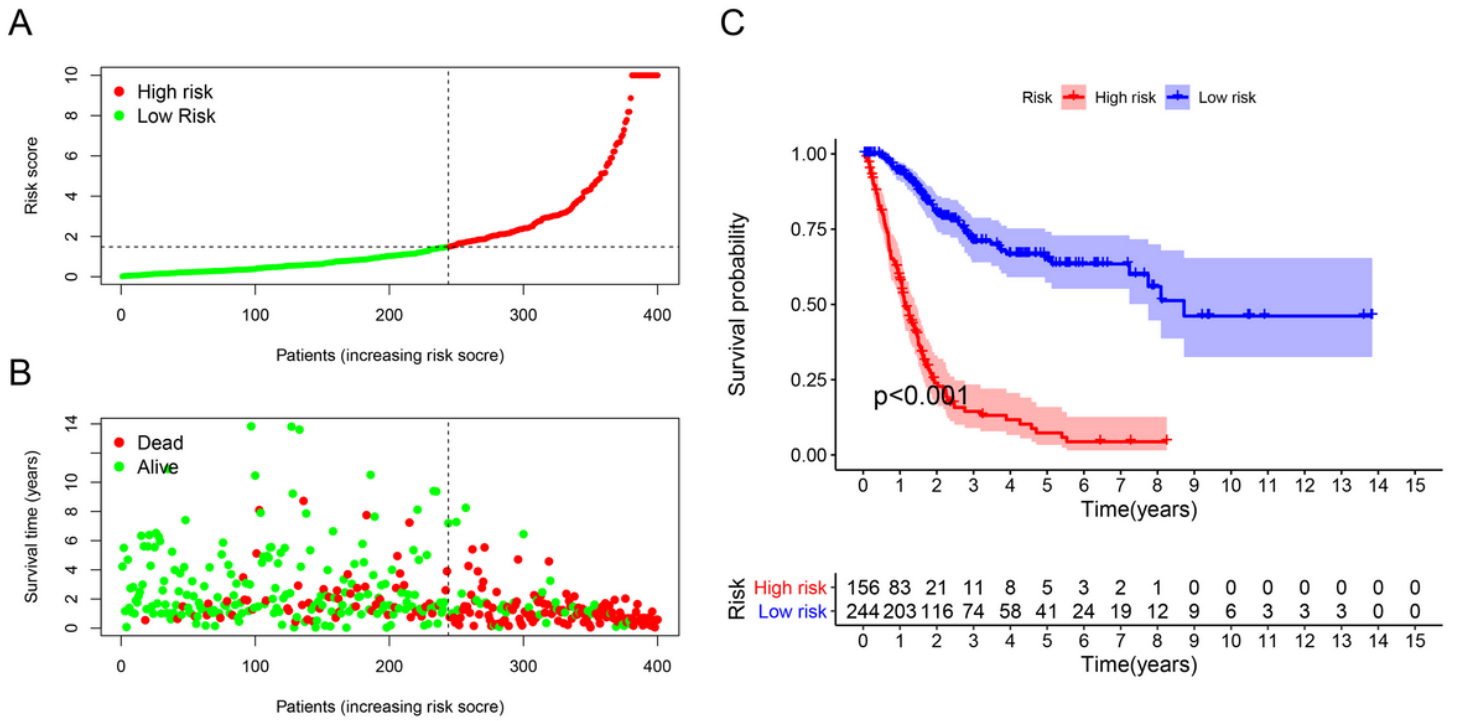


Figure 4

Relationship between the model and patient prognosis. The risk score and survival outcome of each case are shown (A, B). Survival curves of different groups were plotted using the Kaplan–Meier method (C).

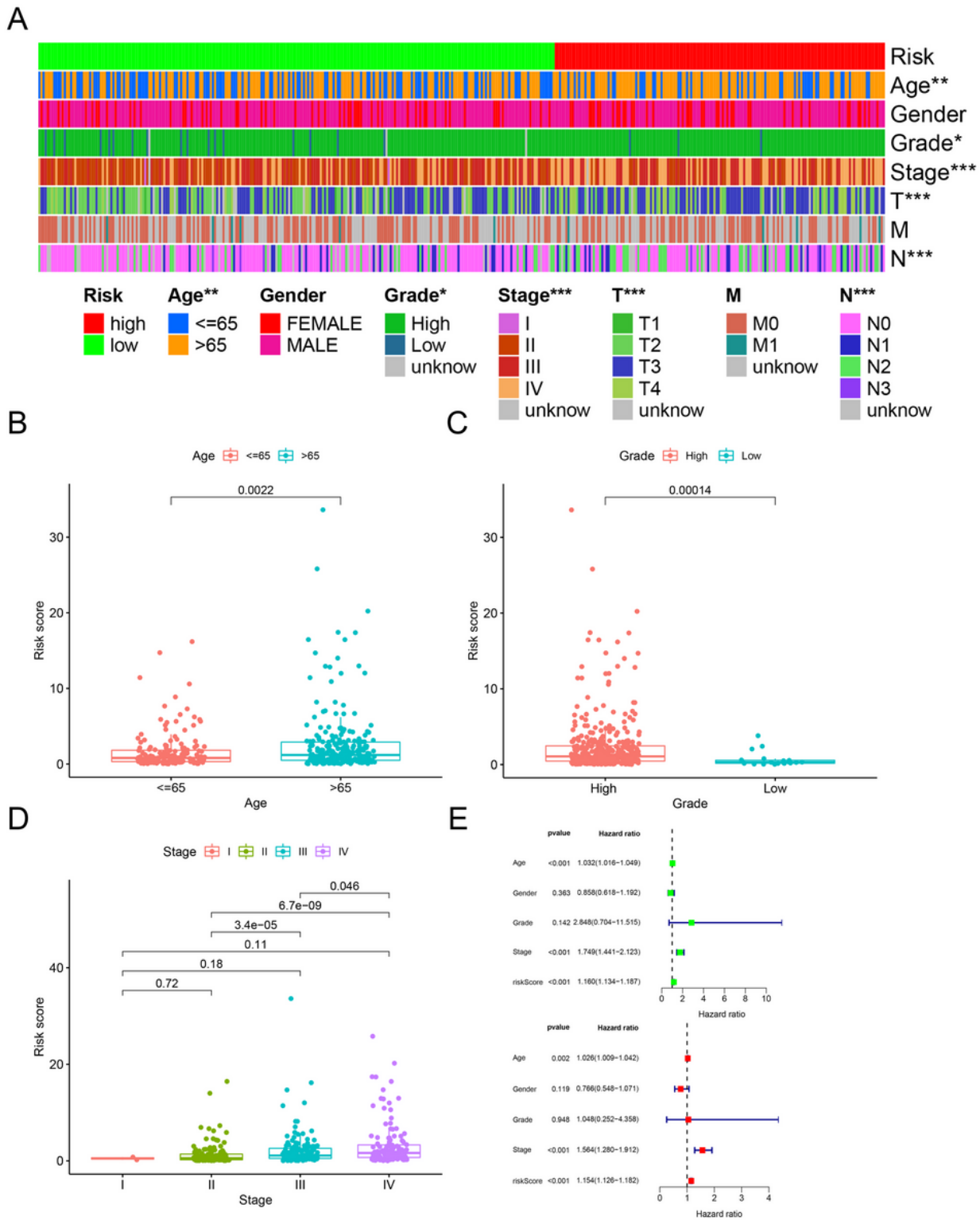


Figure 5

Strip chart (A) and scatter diagrams showing that age (B), grade (C), and tumor stage (D) are significantly related to the RiskScore. The univariate Cox regression model analysis showed that stage ($P < 0.001$), age ($P < 0.001$), and RiskScore ($P < 0.001$) (E) were statistically different, which was further verified by multi-Cox regression model analysis.

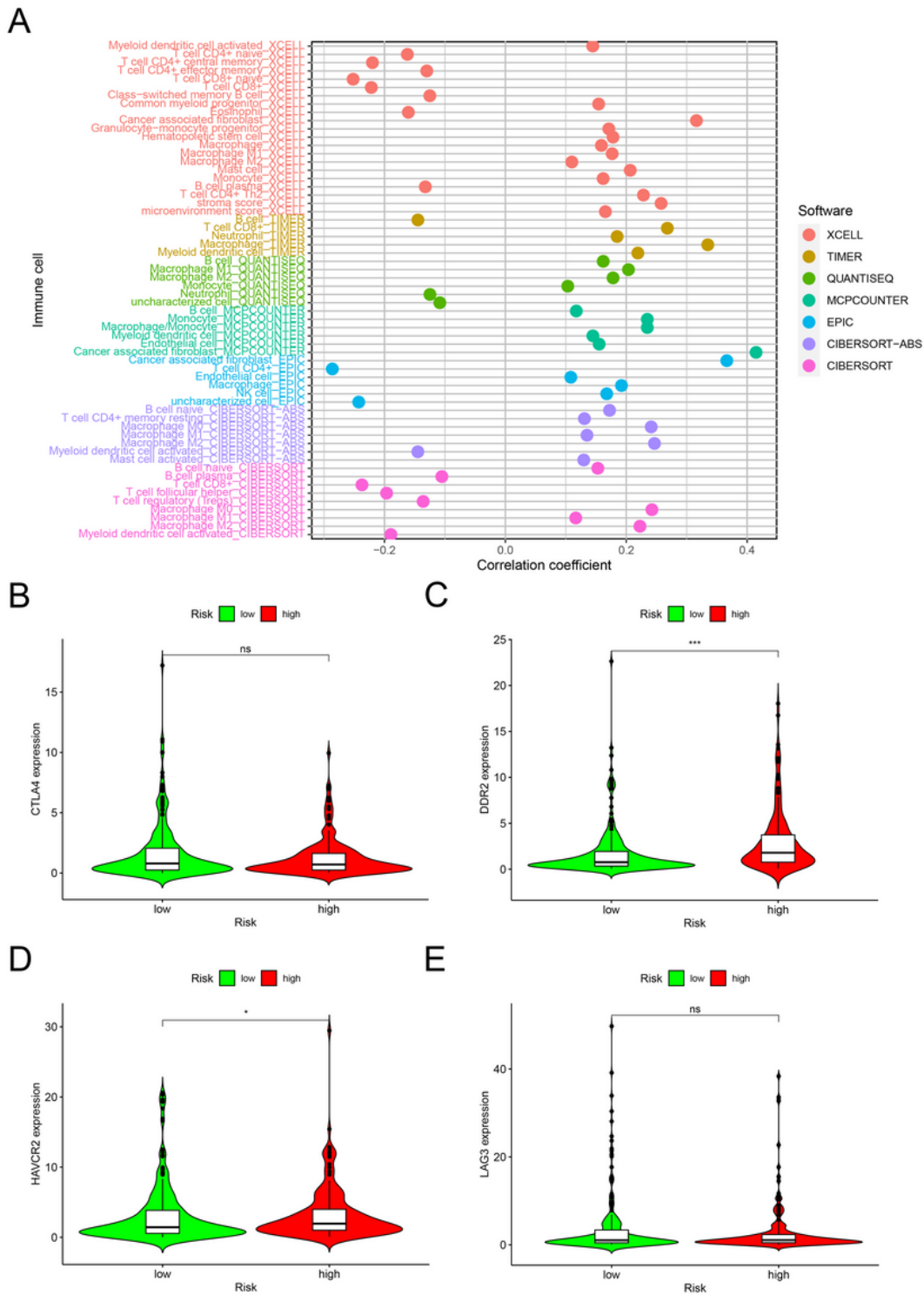


Figure 6

Spearman correlation analysis to detect the infiltration of different immune cells (A). High risk scores were positively correlated with upregulated expression of DDR2 (C), HAVCR2 (D), whereas LAG3 (E), and CTLA4 (B) showed no statistical difference in patients with BLCA.

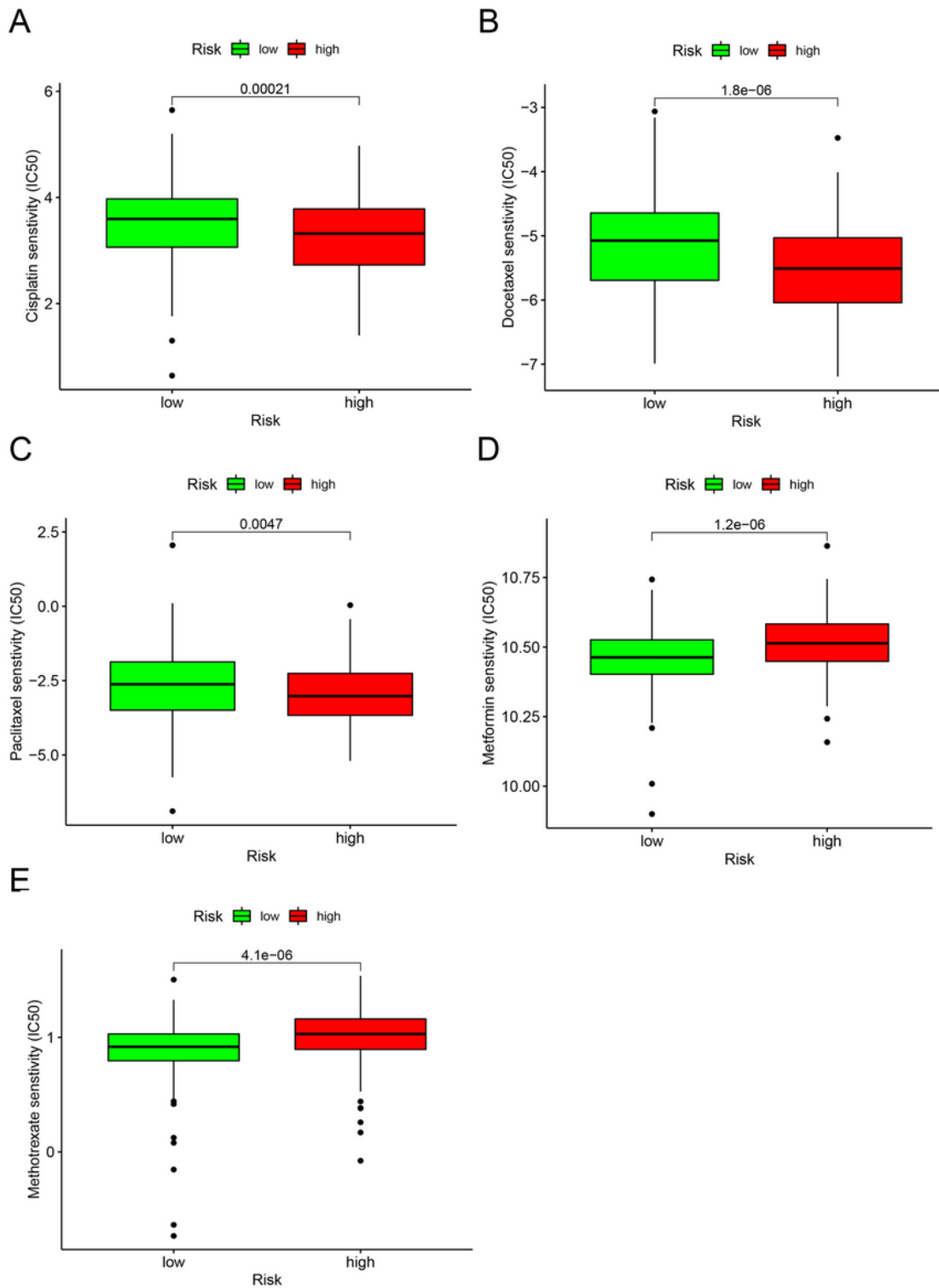


Figure 7

Proposed model can effectively predict chemosensitivity. High risk was related to a lower IC50 for chemotherapeutics, such as doxorubicin, paclitaxel, and cisplatin, whereas was related to a higher IC50 for metformin and methotrexate.